



# Sodium iodate-induced retina degeneration observed in non-separate sclerochoroid/retina pigment epithelium/retina whole mounts

Soo-Young Kim<sup>1,2^</sup>, Yang Zhao<sup>1,3,4</sup>, Hong-Lim Kim<sup>5,6^</sup>, Youngman Oh<sup>7,8^</sup>, Qingguo Xu<sup>1,8,9^</sup>

<sup>1</sup>Department of Pharmaceutics, Virginia Commonwealth University, Richmond, VA, USA; <sup>2</sup>Department of Biology, Virginia Commonwealth University, Richmond, VA, USA; <sup>3</sup>Department of Glaucoma, Aier School of Ophthalmology, Central South University, Changsha, China; <sup>4</sup>Changsha Aier Eye Hospital, Aier Eye Hospital Group, Changsha, China; <sup>5</sup>Department of Anatomy, College of Veterinary Medicine, Konkuk University, Seoul, Republic of Korea; <sup>6</sup>Integrative Research Support Center, Laboratory of Electron Microscope, The Catholic University of Korea, Seoul, Republic of Korea; <sup>7</sup>Department of Pathology, School of Medicine, Virginia Commonwealth University, Richmond, VA, USA; <sup>8</sup>Massey Cancer Center, Virginia Commonwealth University, Richmond, VA, USA; <sup>9</sup>Department of Ophthalmology and Center for Pharmaceutical Engineering and Sciences, Virginia Commonwealth University, Richmond, VA, USA

**Contributions:** (I) Conception and design: SY Kim; (II) Administrative support: SY Kim; (III) Provision of study materials or patients: SY Kim, Y Zhao, HL Kim; (IV) Collection and assembly of data: SY Kim, Y Zhao, HL Kim; (V) Data analysis and interpretation: SY Kim, Y Zhao, HL Kim; (VI) Manuscript writing: All authors; (VII) Final approval of manuscript: All authors.

**Correspondence to:** Soo-Young Kim. ExosomePlus, Inc. #1008, Annex, Seoul St. Mary's Hospital 222, Banpo-daero, Seocho-gu, Seoul, Republic of Korea. Email: gungil@korea.ac.kr.

**Background:** Sodium iodate (SI) is a chemical widely applied to induce retina degeneration in animal models. SI treatment caused formation of rosettes/folds in the outer nuclear layer (ONL) of the rat retina, but it was previously unclear whether SI also forms rosettes in mice. In addition, SI induced retina degeneration was never addressed in non-separate sclerochoroid/retina pigment epithelium/retina whole mount. Here we displayed features of retina degeneration including rosette formation in mice and developed a morphological analytic assessment using sclerochoroid/retina pigment epithelium/retina whole mounts.

**Methods:** SI was intraperitoneally injected in Sprague-Dawley (SD) rats and C57BL/6J mice using a single dose (50 mg/kg) or with a dose range (10 to 50 mg/kg) in BALB/C mice. Rat retinas were investigated up to 2-week post-injection by histology and whole mounts, and mouse retinas were investigated up to 3-week post-injection by histology, fluorescent staining of sections and/or sclerochoroid/retina pigment epithelium/retina whole mounts for the morphological evaluations of the SI-induced retina damage.

**Results:** SI-induced retina damage caused photoreceptor (PR) degeneration and rosettes/folds formation, as well as retina pigment epithelium degeneration and inward migration. It displayed mixed nuclei from choroid to PRs, due to layer disorganization, as shown by single horizontal images in the sclerochoroid/retina pigment epithelium/retina whole mounts. Measurement of the PR rosette area induced by SI provided a quantitative, morphological evaluation of retina degeneration.

**Conclusions:** The method of non-separate sclerochoroid/retina pigment epithelium/retina whole staining and mount allows us to observe the integral horizontal view of damage from sclera to PR layers, which cannot be addressed by using sectioned and separate whole mount methods. This method is applicable for morphological evaluation of retina damage, especially in the subretinal layer.

**Keywords:** Subretina; retina degeneration; rosettes; age-related macular degeneration (AMD)

Received: 02 June 2021; Accepted: 19 August 2021; Published: 15 March 2022.

doi: 10.21037/aes-21-27

View this article at: <https://dx.doi.org/10.21037/aes-21-27>

<sup>^</sup> ORCID: Soo-Young Kim, 0000-0003-3632-8246; Hong-Lim Kim, 0000-0001-6596-6621; Youngman Oh, 0000-0002-7324-2073; Qingguo Xu, 0000-0003-3191-0771.

## Introduction

Retina diseases such as retinitis pigmentosa (RP) and age-related macular degeneration (AMD) have a wide spectrum of pathological features affecting retinal pigment epithelium (RPE), adjacent photoreceptors (PRs) and choroid. RP and AMD are eye disorders with a complex molecular etiology and genetic heterogeneity. While RP results in PR degeneration and peripheral vision loss, caused by genetic mutations, aging is the major contributor to macular RPE degeneration in AMD pathogenesis. There are numbers of chemical-induced animal models for RP and/or AMD retina disorders (1). Among them, sodium iodate (SI) ( $\text{NaIO}_3$ ) is one kind affecting RPE, retina and choroid (2,3) in different animal species, including murine, rabbit and sheep (4).

Since it was introduced in 1941 (5), SI-induced retina damage has been applied widely for both basic and translational studies (6-9). SI is known to directly damage RPE and indirectly manage adjacent PRs. Systemic single injection of SI causes complete destruction of RPE and PR segments and induces macrophage and microglia infiltration in the subretinal space (4,10). However, the pathological features of the ocular damage induced by SI have not yet been explored in sclerochoroid/RPE/retina whole mounts (11,12), which is a recently developed methodology. Here, sclerochoroid/RPE/retina whole mounts were used to examine and characterize the morphological retina degeneration induced by SI. We especially aimed to clarify whether SI-induced the formation of outer nuclear layer (ONL) rosettes/folds in mice. Previously, these rosettes/folds were reported in rats (6,13,14), but still they had not yet been visualized in mice. In this study, we confirmed the formation of ONL folds in Sprague-Dawley (SD) rats, and both C57BL/6J and BALB/C mice. In addition, eyes from BALB/C mice were further examined in non-separate whole mounts of sclerochoroid/RPE/retina to observe the integral degeneration and rosettes formation that occurs when RPE and subretinal to PR layers are not separated. We present the following article in accordance with the ARRIVE reporting checklist (available at <https://aes.amegroups.com/article/view/10.21037/aes-21-27/rc>).

## Methods

### Animals

All studies adhered to the ARVO Statement for the Use of Animals in Ophthalmic and Vision Research and the Animal Research: Reporting of *In Vivo* Experiments.

Animal use and the procedures were approved by the Institutional Animal Care and Use Committees (IACUC) of Virginia Commonwealth University (VCU), USA (No. IACUC AD10001739). The 8- to 10-week-old wild type male SD rats, and C57BL/6J mice and BALB/C mice were used. The rats and mice were maintained at 21–24 °C, with 40–70% humidity and a 12-hour light/dark cycle. Food and water were provided by the institutional animal care facility according to institutional policies. The rats and mice used were randomly divided into each group of control/normal and SI, and then randomly prepared at Day 1 to Week 3 post-SI injection. Maximum four rats and five mice were kept in a cage, and the control/normal group was separated from the SI group. SI (Sigma-Aldrich, USA) solution was prepared in sterile saline, and intraperitoneally injected into both rats and mice at a concentration of 10 to 50 mg/kg. The normal/control group was saline-injected or not injected. A total 64 eyes were examined. The details were as follows (see *Table 1*): SD rat, normal (histology, n=2; whole mount, n=2), SI (histology, n=4; whole mount, n=2); C57BL/6J, normal (histology, n=1; whole mount, n=3), SI (histology, n=1; whole mount, n=5); BALB/C, normal (histology, n=2; fluorescent cryo-section, n=2; whole mount, n=6), SI (10 mg/kg, whole mount, n=6; 20mg/kg, whole mount, n=6; 40 mg/kg, whole mount, n=2; 50 mg/kg, histology, n=3; fluorescent cryo-section, n=7; whole mount, n=10).

### Retinal histology

Eyeballs were fixed in 4% paraformaldehyde (PFA)-PBS until processing, at least over 1 week before dehydrated and embedded in paraffin or post-fixed in 1% osmium tetroxide-PBS before being embedded in epon resin. The retina sections (1 to 4  $\mu\text{m}$ ) were cut perpendicularly and stained with hematoxylin and eosin (H&E) or toluidine blue.

### Fluorescent staining of retina sections

Mouse eyeballs were fixed with 4% PFA-PBS up to 4 hours, and vertical eyeball sections were prepared at 12  $\mu\text{m}$  thickness using a cryostat machine (Leica), and then stored at -80 °C until use. In fluorescent staining, the retina sections were the first permeabilized and blocked for 15 min with 1% bovine serum albumin (BSA) and 0.2% Triton X-100 in PBS. Primary and secondary antibodies were each applied for 1 hour and 30 min, each at room temperature (RT), in a 1:1,000 dilution. The following

antibodies were used: mouse monoclonal anti-RPE65 (Life Technologies, catalog number: MA1-116578) and relevant secondary antibodies conjugated with Alexa Fluor 488 (Life Technologies). Nuclei were counterstained with Hoechst 33342 (Life Technologies, catalog number: H3570).

#### ***Terminal deoxynucleotidyl transferase-mediated dUTP nick end labelling (TUNEL) labelling***

TUNEL (Roche Diagnostics) was applied to detect dying cells in retina sections according to the manufacturer's instruction. Cryo- and paraffin-retina sections were incubated with terminal deoxynucleotidyl transferase and fluorescein-dUTP for 1.5 hours. Paraffin-sections were pre-treated by proteinase K (1 µg/mL, Sigma-Aldrich) before TUNEL labelling.

#### ***Sclerochoroid/RPE/retina whole mount***

Eyeballs were fixed in 4% PFA-PBS for 1–2 hours. The anterior segment and lens were removed from the eyeballs. The sclerochoroid/RPE/retina tissues were stained with phalloidin 488 (Life Technologies, catalog number: A12379), RPE65 and/or Hoechst 33342 and mounted on glass slides with the upside of sclerochoroid facing outward for confocal scanning of subretinal and neighboring layers. The pigmented sclerochoroid/RPE/retina tissues from C57BL/6J were bleached by hydrogen peroxide (Sigma-Aldrich) before staining (11,15).

#### ***Microscopy***

Histology sections were photographed using an Olympus microscope (Olympus Optical CO., LTD., Japan). Fluorescent stained/labelled slides of retina sections and whole mounts were imaged by single, z-stack and/or tiled scan using a Zeiss 700 confocal microscope (Carl Zeiss Meditec, Germany).

#### ***Image processing and area quantification of rosettes***

For the measurement of rosettes areas, the horizontal view of PR layer in sclerochoroid/RPE/retina whole mounts was tile-scanned with z-stacks under 10X objective lens and projected. First the optic nerve head was center-XY positioned, and the area was focused and center-Z positioned. Second, while defining the tile regions to cover all areas of the whole mounts, several local areas

were focused to verify the z range, and two local areas were chosen to define the first and last of Z position. The acquisition of 8×8 tiles and 3 z-slices, under a 10× objective lens, covered the areas of interest in the retina whole mounts, including the ONL depth. The images were stitch-processed and projected into a single image for quantification of rosettes. A square area, with 2.5 mm width and length, centered to the optic nerve head of the projected images, was used (Figure S1). The retinal area and rosettes were selected, and colored black in each layer of the Photoshop files. The areas of retina and rosettes were then measured using the particle analyzing tool of ImageJ. For the retina area, non-retinal areas were excluded from the 2.5 mm × 2.5 mm squares. The total areas of rosettes in the selected retina area were obtained. Next, the total areas of rosettes per unit region (6 mm<sup>2</sup>) and the area ratio of the occupied rosettes in the retinal region were calculated. The data (means ± SEM) were graphed with GraphPad Prism. Rosette areas were quantified from six eyeballs of normal, four eyeballs of Week 1 and three eyeballs of Week 3. One eyeball allotted for the whole mount of Week 3 (Table 1) was excluded in the quantitation because part of eyeball was scarred by poor scissor handling.

#### ***Statistical analysis***

The data were graphed and analyzed with GraphPad Prism. Data were given as the means ± SEM. P<0.05 was considered statistically significant (two-tailed unpaired *t*-test).

## **Results**

### ***The histological examination of SI-induced retina degeneration in SD rats, C57BL/6J and BALB/C mice***

A single intraperitoneal injection of 50 mg/kg of SI was applied to induce RPE and PR degeneration in SD rats, C57BL/6J and BALB/C mice (Figure 1), since the most commonly used dose of SI in murine is 40 to 50 mg/kg (10). In normal retina sections, there are continuously organized RPE, outer and inner segment (OS/IS) layers of PRs, and smooth-lined outer limiting membrane (OLM, orange arrow heads, Figure 1A,1C,1E) between the ONL and subretinal space. However, in SI-damaged retinas, there were loss of RPE cell nuclei, dislocation and/or swellings of RPE cells (arrows), disruption of PR segments and disorganized ONL (asterisks). The retina rosettes/folds were distinctly and consistently observed in all

**Table 1** Eyeballs used in this study

Groups (total eyeballs)	Does (mg/kg)	Purposes	Days/weeks	No. of eyes
SD rats				
Normal [4]	–	Histology	–	2
		Whole mount	–	2
SI [6]	50	Histology	Week 1	2
			Week 2	2
		Whole mount	Week 1	2
C57BL/6J mice				
Normal [4]	–	Histology	–	1
		Whole mount	–	3
SI [6]	50	Histology	Week 1	1
		Whole mount	Week 1	3
			Week 3	2
BALB/C mice				
Normal [10]	–	Histology	–	2
		Fluorescent	–	2
		Whole mount	–	6
SI [34]	10	Whole mount	Day 1	2
			Week 1	2
			Week 3	2
	20	Whole mount	Day 1	2
			Week 1	2
			Week 3	2
	40	Whole mount	Week 1	2
	50	Histology	Week 1	1
			Week 3	2
			Fluorescent	Day 1
		Whole mount	Week 1	1
Week 2			2	
Week 3			2	
	Whole mount	Day 1	2	
		Week 1	4	
		Week 3	4	

SD, Sprague-Dawley; SI, sodium iodate.

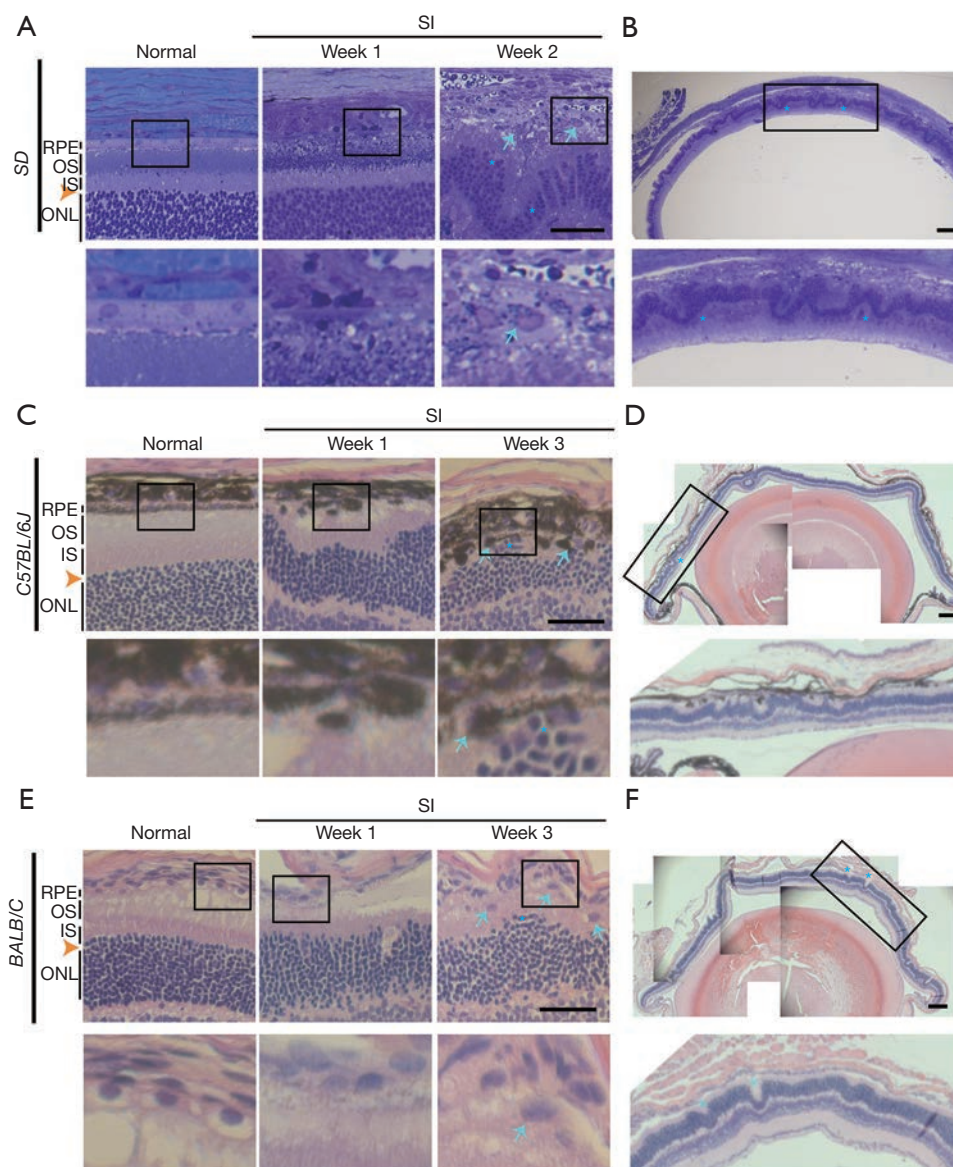


**Figure 1** Histological examination of SI-induced retina damage in SD rats, C57BL/6J and BALB/C mice. Animals were peritoneally (i.p.) injected with SI (50 mg/kg). (A) Representative images of normal and SI-damaged retinas of SD rats at Week 1 and Week 2, post SI injection. (B) ONL disorganization in SI-damaged retina of SD rats at Week 2. (C) Normal and SI-damaged retinas of C57BL/6J mice at Week 1 and Week 3. (D) ONL disorganization of SI-damaged retinas of C57BL/6J mice at Week 1. (E) Normal and SI-damaged retinas of BLAB/C mice at Week 1 and Week 3. (F) ONL disorganization of SI-damaged retinas of BLAB/C mice at Week 1. All boxed areas in (A-F) are shown with 3× magnification, below each image. Asterisks (A-F) indicate ONL disorganization. Arrows (A,C,E) indicate swelled RPE cells. Orange arrow heads at the left side (A,C,E) indicate the OLM. Toluidine blue (A,B) and hematoxylin and eosin (H&E) staining (C-F). Scale bars: 50  $\mu$ m in (A,C,E); 200  $\mu$ m in (B,D,F). SI, sodium iodate; SD, Sprague-Dawley; RPE, retina pigment epithelium; OS, outer segment; IS, inner segment; ONL, outer nuclear layer; OLM, outer limiting membrane.

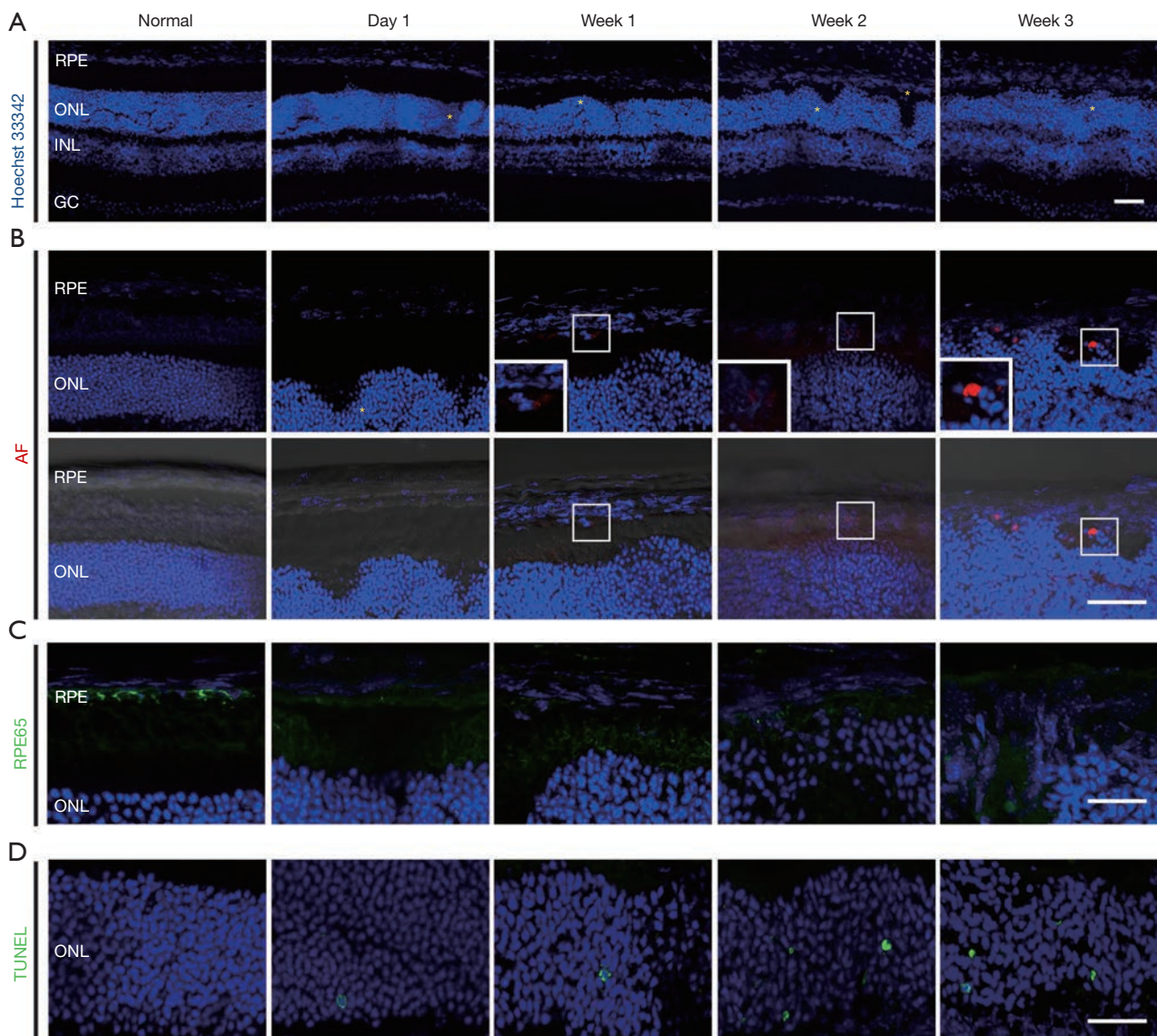


**Figure 2** Vertical fluorescent examination of SI-induced retina damage from Day 1 to Week 3. SI (50 mg/kg, i.p.)-induced retina degeneration in BALB/C mice. (A) Disorganization (asterisks) of retina layers, stained by Hoechst 33342. (B) AF signals in SI-damaged retinas in BALB/C mice. The panel below is overlaid DIC images. Boxed areas are magnified in the inserts. (C) Retina sections stained by RPE65 primary and Alexa Fluor 488 secondary antibodies. (D) Retina sections stained by TUNEL. Asterisks (A,B) indicate ONL disorganization. Scale bars: 50  $\mu$ m in A; 25  $\mu$ m in (B-D). RPE, retina pigment epithelium; ONL, outer nuclear layer; INL, inner nuclear layer; GC, ganglion cell layer; AF, autofluorescence; SI, sodium iodate; DIC, differential interference contrast.

retina histological sections of SI-injected SD rats, C57BL/6J mice and BALB/C mice (asterisks, *Figure 1B,1D,1F*). In the frozen sections of SI-damaged BALB/C retinas, the ONL disorganization was observed even on Day 1 after SI-injection (*Figure 2A-2D*). Additionally, autofluorescence (AF) signals were minor by Week 2, but became stronger at Week 3 after

SI-injection (*Figure 2B*). The expression of RPE65, a marker of RPE, was not observed in the RPE layer even on Day 1 after SI-injection (*Figure 2C*), indicating that SI induces RPE degeneration before Day 1, whereas dying cells in ONL were increasingly observed from Day 1 to Week 3 (*Figure 2D*).

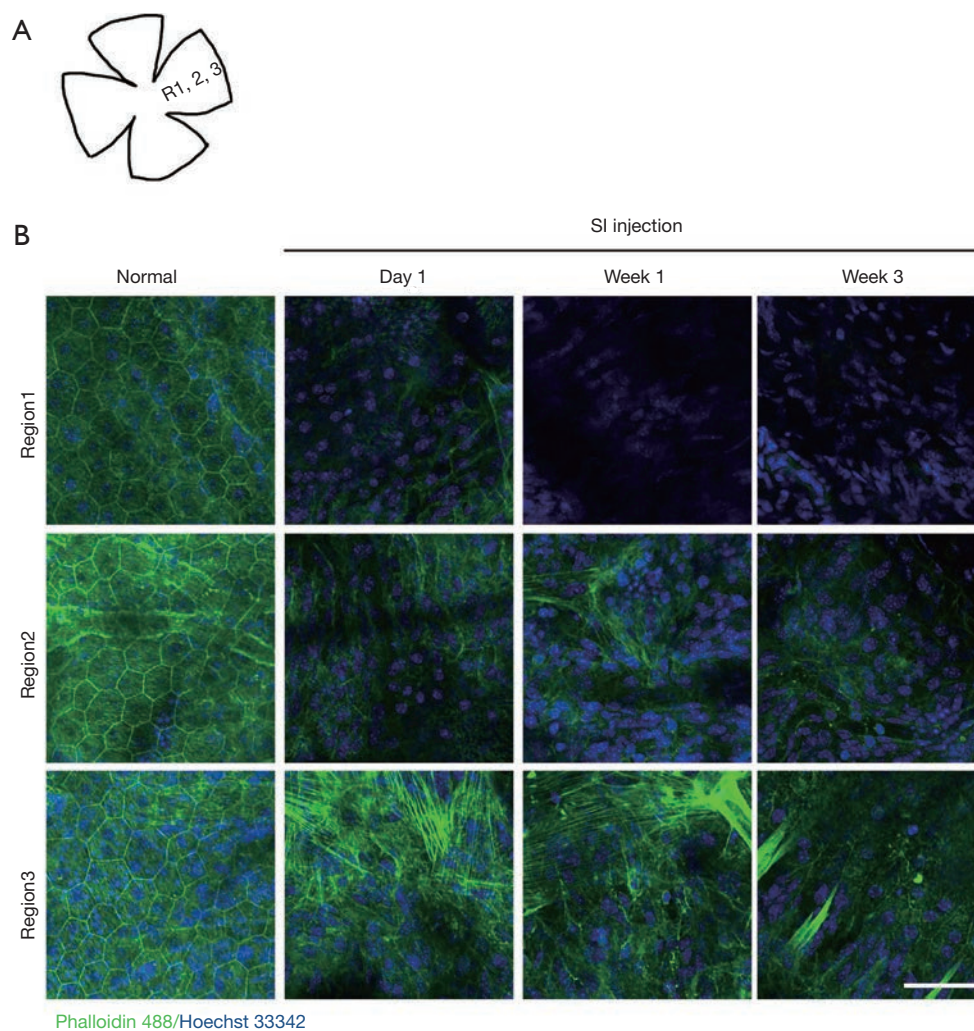


**Figure 3** RPE degeneration in horizontal view of whole mounts. SI (50 mg/kg, i.p.)-induced RPE degeneration in BALB/C mice. (A) A schematic image of quadrant whole mount with regional indication from center (R1) to peripheral region (R3). R1 is near to optic nerve head and R3 is outside the muscle, and R2 is between R1 and R3. (B) Sclerochoroid/RPE/retina whole mounts were stained with Alexa 488-conjugated phalloidin and Hoechst 33342. Images were taken of RPE layers from center (R1) to peripheral (R3) retinas at Day 1, Week 1 and Week 3. Scale bar: 50  $\mu$ m. SI, sodium iodate; RPE, retina pigment epithelium.

#### *SI-induced retina damage observed from choroid, RPE to PR layers in sclerochoroid/RPE/retina whole mounts*

Sclerochoroid/RPE/retina whole mount staining of phalloidin 488 was applied to observe features in the horizontal view of the vertical histology and fluorescent staining described in *Figures 1,2*. SI-induced RPE damage was observed in the central region (R1) of whole mounts with any doses studied (*Figure 3* and *Figure S2*), and the peripheral RPE damage was consistently induced by 50 mg/kg SI. At this concentration, there was no visible hexagonal

or octagonal RPE, and a total loss of RPE monolayer occurred through the whole posterior region of the eyeballs (R1 to R3) from Day 1 to Week 3 (*Figure 3B*). In contrast, low doses of SI (10 and 20 mg/kg) induced only central RPE degeneration (*Figure S2*). The dose of 40 mg/kg SI inconsistently induced peripheral RPE degeneration; a border between the RPE degenerated and relatively healthy regions was peripherally observed (*Figure 4A*). RPE65 expression was not present in the damaged region of RPE layer, but in the less damaged area of RPE layer, RPE65-positive cells were observed (*Figure 4A*, arrow heads). The

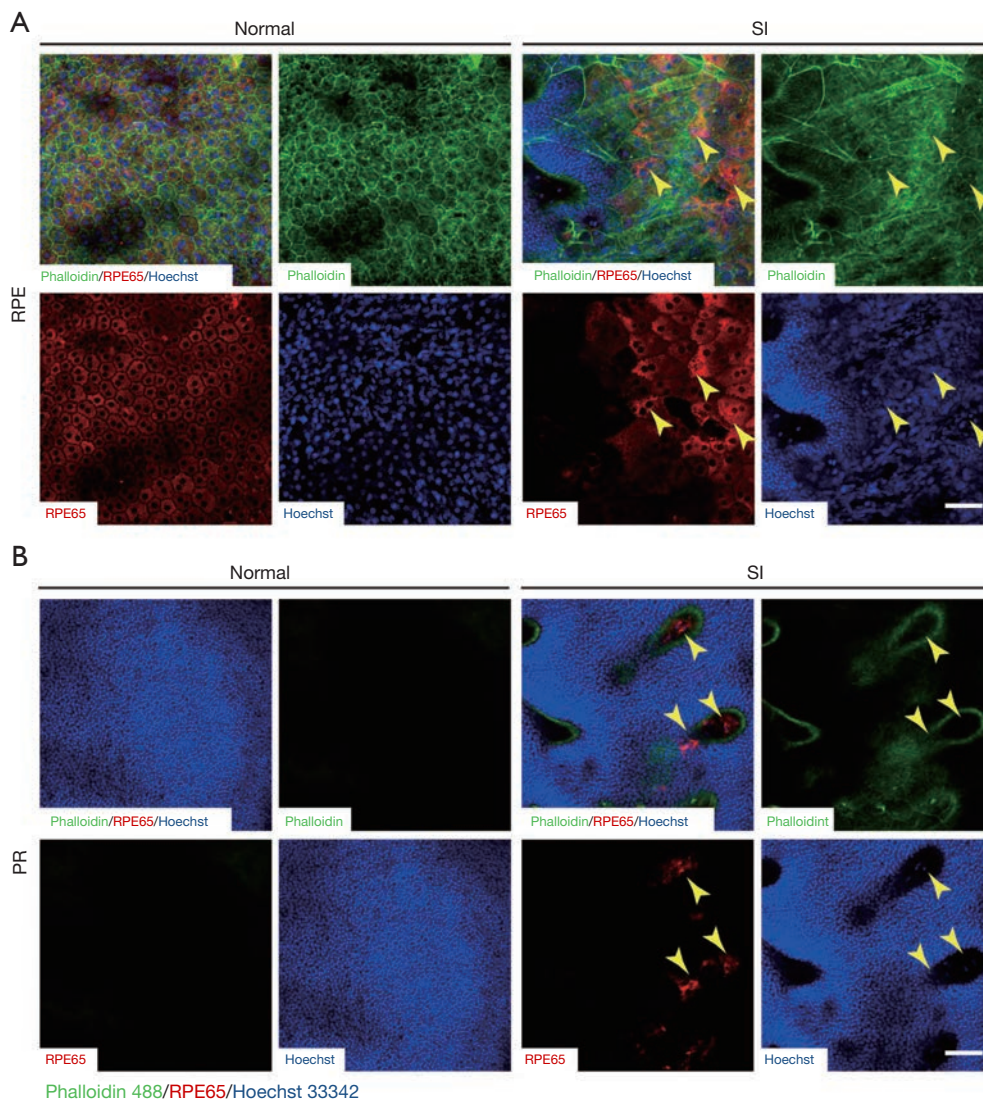


**Figure 4** SI-induced RPE and ONL degeneration in sclerochoroid/RPE/retina whole mounts stained with Alexa 488-conjugated phalloidin (green) and RPE65 (red). SI (40 mg/kg, i.p.)-induced degeneration in retinal pigment epithelium (A) and photoreceptor (B) layers of BALB/C mice. RPE65 expression (arrow heads) was observed at the bordered region of RPE damage and ONL (PR) layer. Scale bars: 50  $\mu\text{m}$ . SI, sodium iodate; RPE, retina pigment epithelium; PR, photoreceptor; ONL, outer nuclear layer.

RPE cell size stained by RPE65 and outlined by phalloidin staining appeared bigger than the normal cells (*Figure 4A*), indicating RPE cell extension/swelling, which was also observed in histology (*Figure 1*). RPE65-positive cells were rarely observed even at ONL, PR layer (*Figure 4B*, arrow heads), and the inward moving RPE65-positive cells were not stained by phalloidin. The morphology of intra-retinal migrating RPE cells was also not epithelium, suggesting an epithelial to mesenchymal transition of RPE cells, similar to a report from another SI-induced retina damage (13). Further,

activated RPE migration has been reported in human AMD as an early AMD phenotype (16,17) and in rat SI-damaged retina (13).

In a series of confocal z images of sclerochoroid/retina/RPE whole mounts with a 2  $\mu\text{m}$ -interval (*Figure 5*), normal retinas displayed choroidal vasculature (asterisks) in the choroid layer (panels A,B) and RPE monolayer (panel C), and there were no nuclei in the PR segment layer (panel D). On the other hand, SI-damaged retinas exhibited single z horizontal images mingled with different types of cell

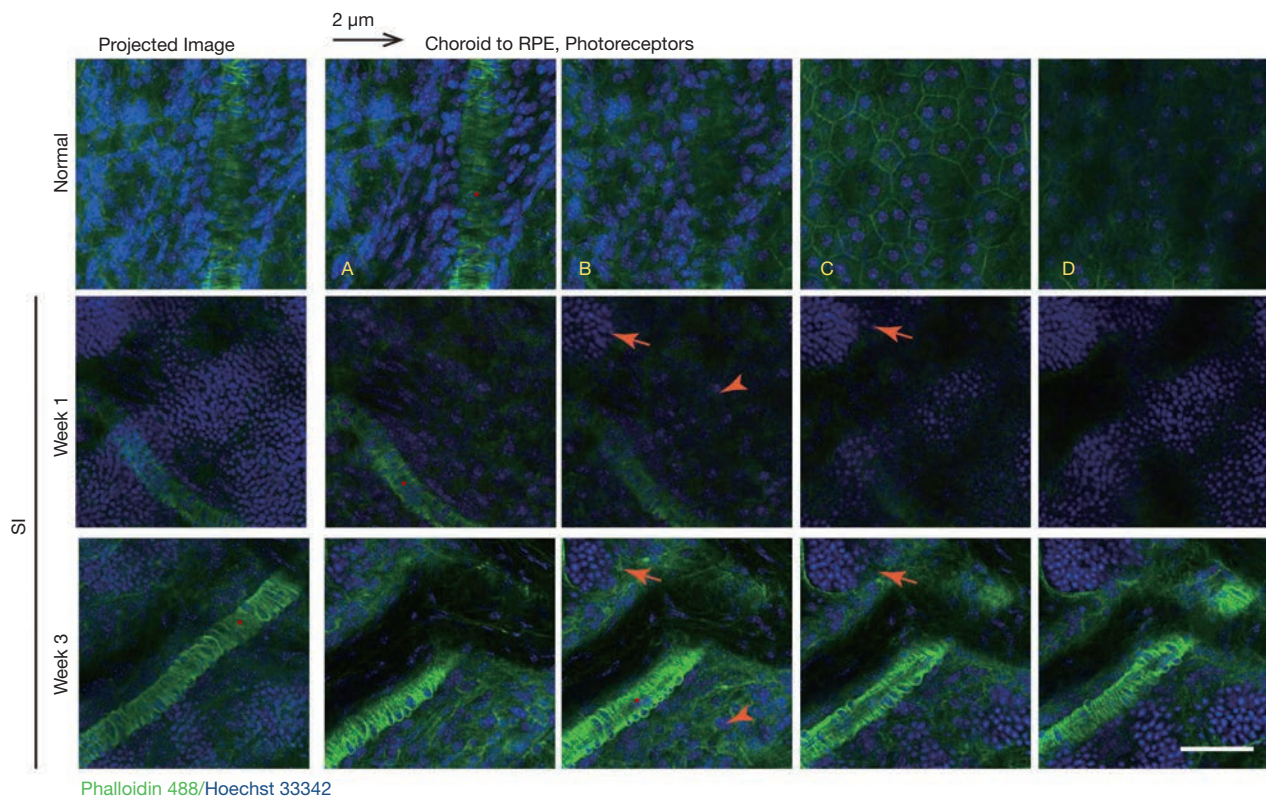


**Figure 5** SI-induced ocular damage from choroid toward ONL in sclerochoroid/RPE/retina whole mounts stained with Alexa 488-conjugated phalloidin. SI (50 mg/kg, i.p.)-induced retina degeneration in BALB/C mice. Images were arranged at a 2  $\mu\text{m}$  interval with projected images (the most left column). The separate distinct layers of choroid (A,B), RPE (C), PR segment (D) in normal are blended in SI retinas. PR nuclei (arrows) and RPE nuclei (arrow heads) in SI-damaged retinas. Choroidal vasculatures (asterisks) in normal and SI-damaged retinas. Scale bar: 50  $\mu\text{m}$ . RPE, retina pigment epithelium; SI, sodium iodate; ONL, outer nuclear layer; PR, photoreceptor.

nuclei from choroid, RPE and ONL (Figure 5, middle and lower panels). Additionally, there were islands of PR nuclei (arrows), choroid vessels (asterisks) and apparent RPE nuclei (arrow heads) observed in single z images. Another blue channel separation of Hoechst 33342 in the confocal images of sclerochoroid/RPE/retina whole mounts (Figure 6) demonstrated loss of the RPE layer and apparent dislocation of RPE nuclei. RPE nuclei in the boxed areas were magnified in the inserts for the clear observation. PR rosette formation (arrows) was also clearly observed. The features of RPE degeneration, RPE movement and PR rosettes formation, and the disorganized subretinal and neighboring layers were also observed in C57BL/6J sclerochoroid/RPE/retina whole mounts (Figure S3).

#### *SI-induced PR rosette quantification in the tiled confocal images of sclerochoroid/RPE/retina whole mounts*

The SI-induced ONL rosettes were scanned in the tiled confocal images and the occupied rosettes areas per unit retinal region were quantified. The area ratios of the rosettes in a retinal region were calculated and graphed (Figure S1 and Figure 7). The titled ONL images of the sclerochoroid/RPE/retina whole mounts were taken under 10X objective lens through whole regions of eyeball, with z-scanning, and the projected images were obtained. SI with low doses (10 and 20 mg/kg, i.p.) induced center RPE degeneration (Figure S2), but did not induce ONL rosettes (20 mg/kg—Figure 7 and 10 mg/kg—data not shown). For the ONL rosette quantification (Figure S1), the center

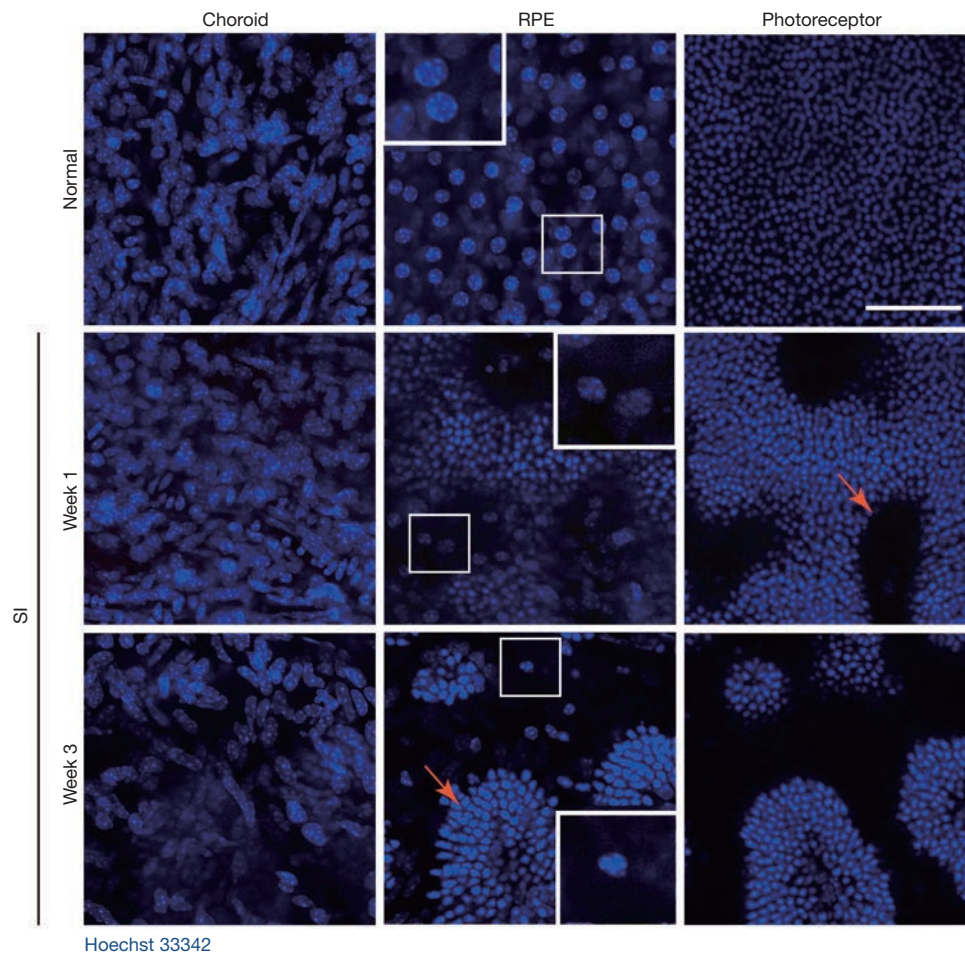


**Figure 6** Hoechst staining of SI-induced ocular damage at the level of choroid, RPE and PR layers in sclerochoroid/RPE/retina whole mounts. SI (50 mg/kg, i.p.)-induced retina degeneration in BALB/C mice results in PR rosettes (arrows) and RPE nuclei (boxed areas). Higher magnification of RPE nuclei in the boxed areas are shown in the inserts. Scale bar: 50  $\mu\text{m}$ . RPE, retina pigment epithelium; SI, sodium iodate; PR, photoreceptor.

regions (2.5 mm width and length) were obtained from the projected tile-scanned ONL confocal images, and then the retinal area, and the rosettes inside, were selected and filled with black color in the separate layers of Photoshop. The retina area and rosette areas were measured by particle analysis in ImageJ. The quantified values of total rosette area per unit retina region were an average of  $201.82 \pm 24.73$  ( $\times 1,000 \mu\text{m}^2$ , SEM,  $n=4$ ) at Week 1 and an average of  $188.94 \pm 15.36$  ( $n=3$ ) at Week 3, after SI-injection. The occupied area ratios of rosettes in the retinal region measured were an average of  $3.36 \pm 1.65$  (SEM) at Week 1 and an average of  $3.15 \pm 0.77$ . We did not find any significant difference of the rosette area and the occupied area ratio of rosettes in the retinal region between Week 1 and Week 3.

## Discussion

SI has been extensively applied to induce retina damage as an animal model platform for geographic atrophy AMD in different species including murine (4,5), via the several different routes of intravenous, intraperitoneal, retro-orbital, intravitreal and subretinal injections (4,7,8,10,18). However, the SI-formed ONL undulations referred to as rosettes/folds were not clearly described and reported in mice. Here, we used non-separate sclerochoroid/RPE/retina whole mounts to maintain retina layer integrity, and observed RPE degeneration, RPE inward movement, retinal layer dislocation, PR degeneration and ONL rosettes from a new vantage point. We also found SI-induced ONL rosettes in

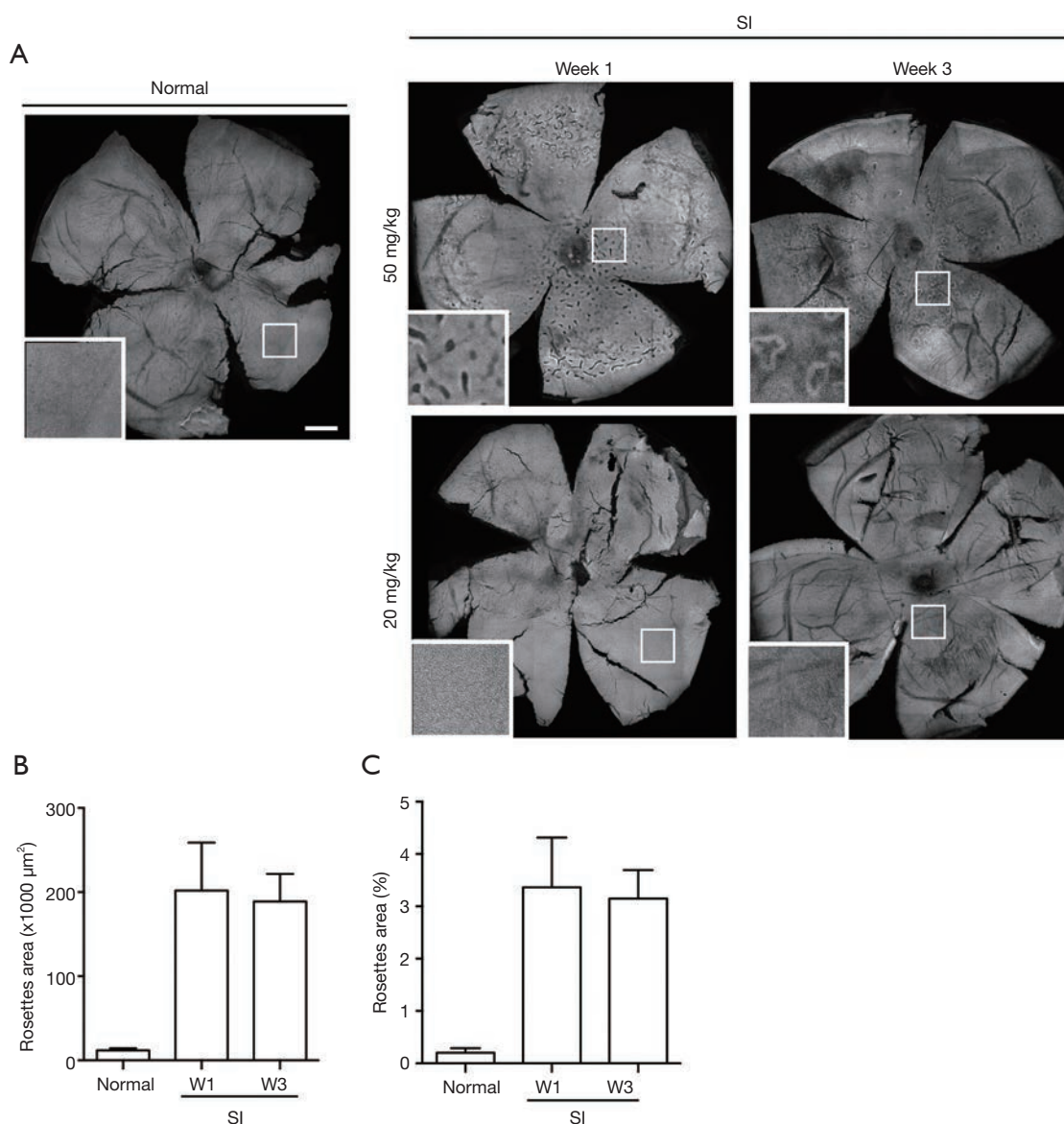


**Figure 7** Quantification of SI-induced ONL rosette formation in sclerochoroid/RPE/retina whole mounts. SI (20, 50 mg/kg, i.p.)-induced retina degeneration in BALB/C mice. (A) The tiled and projected confocal images of Normal, Week 1 and Week 3, post SI injection. Boxed areas are magnified in inserts. (B) A graph of total areas of rosettes in the defined retina area at Week 1 and Week 3 (see details in [Figure S1](#)). (C) A graph of the area ratio of occupied rosettes in retinal regions. Scale bar, 500 μm. SI, sodium iodate; ONL, outer nuclear layer; RPE, retina pigment epithelium.

C57BL/6J as well as BLAB/C mice. However, we initially hypothesized that SI would induce rosette formation in BLAB/C mice, we thought it might not in C57BL/6J, based on published literature, because BLAB/C mice display distinct fundus AF (FAF) compared to C57BL/6J (10), and FAF can be caused by rosettes.

A detailed investigation on the reason why FAF was

distinct in BLAB/C is beyond the purpose of this study, but we suspect that the reason of distinct FAF in SI-damaged retina of BLAB/C mice might be due to a difference in the severity of degeneration and/or AF. SI makes the retina of C57BL/6J mice thin quickly, resulting in the disappearance of formed rosettes, while less severe retina degeneration in BLAB/C might maintain rosettes for a longer period

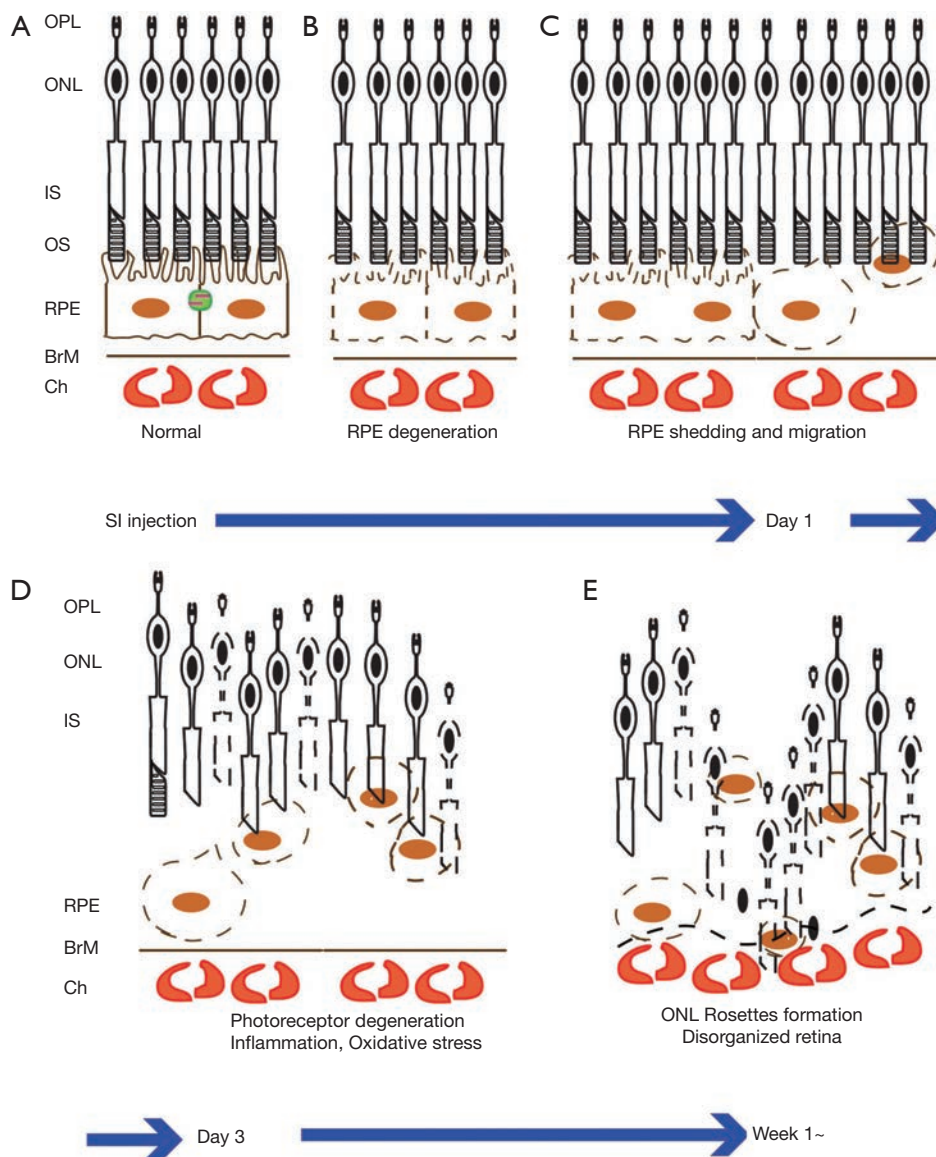


**Figure 8** Schematic summary of ocular degeneration in SI-induced retina degeneration. (A) Normal retina layers. (B) RPE degeneration starts before the end of Day 1. (C) RPE loss and RPE intraretinal migration at Day 1. (D) Progressing PR degeneration following RPE degeneration. (E) ONL rosettes formation and disrupted subretinal space with mingled cells from neighboring layers. OPL, outer plexiform layer; ONL, outer nuclear layer; IS, inner segment; OS, outer segment; PR, photoreceptor; RPE, retinal pigment epithelium; BrM, Bruch's membrane; Ch, choroid; SI, sodium iodate.

of time, and there might be different microglia and macrophages recruited, causing AF. We were more focused on observing SI-damaged retinas in non-pigmented BALB/C mice using sclerochoroid/RPE/retina whole mounts, because, in the whole mount method, the pigmented eyeballs needed melanin bleaching, and with this step, phalloidin staining was hindered. In the future, it will be advantageous to validate the

compatibility of other types of antibody staining, such as ZO-1 and cadherins, to outline the RPE cells when a bleaching step in sclerochoroid/RPE/retina whole mount preparation of pigmented mice is necessary. In the retina degeneration observed in SI-high doses (40–50 mg/kg, i.p.) (Figure 8), SI-systemic injection induces acute RPE degeneration before Day 1, and slower PR damage from Day 1 to Week 3, before

forming distinct ONL rosettes/folds around Week 1. In damaged RPE layer, RPE65 expression dramatically disappeared, only occasionally were migrating ectopic RPE cells that maintained RPE65 expression still visible. The RPE cells that migrated intraretinally in this and previous SI-AMD model studies (13) might represent the clinically observed RPE inward movement at early and intermediate AMD stages before GA (16,17). Rosette formation, a feature of retinal degeneration induced by SI-injection has also been observed in human cases of RP and retinal detachment (19-21). Considering that SI induces either PR or RPE degeneration, or both PR and RPE degeneration, as well as choroid degeneration depending on the injection routes and dosages (7,8,22), the SI-induced retina degeneration model could be used to represent different stages and classes of human geographic atrophy AMD. Finally, in addition to provides a quantification method to measure ONL rosette morphology, this study contribute to the better understanding of how SI-induced retina degeneration progresses and affects choroid, RPE, subretina and PRs, by using intact sclerochoroid/RPE/retina whole mounts.

## Acknowledgments

We would like to thank Dr. Gail Seabold (NIH Office of Intramural Training and Education, National Institutes of Health) for critical reading and manuscript editing. We are grateful for the use of Animal and Imaging Facilities, Virginia Commonwealth University and Konkuk University. *Funding:* This work was partly supported by the National Institutes of Health (R01EY027827, QX) and VCU (VETAR 2021, YO) grants. There was no role of the funders in the design, analysis or reporting of the study.

## Footnote

*Reporting Checklist:* The authors have completed the ARRIVE reporting checklist. Available at <https://aes.amegroups.com/article/view/10.21037/aes-21-27/rc>

*Data Sharing Statement:* Available at <https://aes.amegroups.com/article/view/10.21037/aes-21-27/dss>

*Peer Review File:* Available at <https://aes.amegroups.com/article/view/10.21037/aes-21-27/prf>

*Conflicts of Interest:* All authors have completed the ICMJE uniform disclosure form (available at <https://aes.amegroups.com/article/view/10.21037/aes-21-27/coif>).

YO reports that this study had received VCU VETAR 2021 grants. QX reports that this study was partly supported by the National Institutes of Health (R01EY027827). SYK reports that he is an employee of ExosomePlus. Inc. The other authors have no conflicts of interest to declare.

*Ethical Statement:* The authors are accountable for all aspects of the work in ensuring that questions related to the accuracy or integrity of any part of the work are appropriately investigated and resolved. All studies adhered to the ARVO Statement for the Use of Animals in Ophthalmic and Vision Research and the Animal Research: Reporting of *In Vivo* Experiments. Animal experiments were performed under animal protocols approved by the Institutional Animal Care and Use Committees of Virginia Commonwealth University and Konkuk University (No. IACUC AD10001739).

*Open Access Statement:* This is an Open Access article distributed in accordance with the Creative Commons Attribution-NonCommercial-NoDerivs 4.0 International License (CC BY-NC-ND 4.0), which permits the non-commercial replication and distribution of the article with the strict proviso that no changes or edits are made and the original work is properly cited (including links to both the formal publication through the relevant DOI and the license). See: <https://creativecommons.org/licenses/by-nc-nd/4.0/>.

## References

1. Kim SY, Kambhampati SP, Bhutto IA, et al. Evolution of oxidative stress, inflammation and neovascularization in the choroid and retina in a subretinal lipid induced age-related macular degeneration model. *Exp Eye Res* 2021;203:108391.
2. Zieger M, Punzo C. Improved cell metabolism prolongs photoreceptor survival upon retinal-pigmented epithelium loss in the sodium iodate induced model of geographic atrophy. *Oncotarget* 2016;7:9620-33.
3. Machalińska A, Lubiński W, Kłos P, et al. Sodium iodate selectively injures the posterior pole of the retina in a dose-dependent manner: morphological and electrophysiological study. *Neurochem Res* 2010;35:1819-27.
4. Kannan R, Hinton DR. Sodium iodate induced retinal degeneration: new insights from an old model. *Neural Regen Res* 2014;9:2044-5.

5. Sorsby A. Experimental pigmentary degeneration of the retina by sodium iodate. *Br J Ophthalmol* 1941;25:58-62.
6. Xiao J, Yao J, Jia L, et al. Protective Effect of Met12, a Small Peptide Inhibitor of Fas, on the Retinal Pigment Epithelium and Photoreceptor After Sodium Iodate Injury. *Invest Ophthalmol Vis Sci* 2017;58:1801-10.
7. Bhutto IA, Ogura S, Baldeosingh R, et al. An Acute Injury Model for the Phenotypic Characteristics of Geographic Atrophy. *Invest Ophthalmol Vis Sci* 2018;59:AMD143-51.
8. Ahn SM, Ahn J, Cha S, et al. The effects of intravitreal sodium iodate injection on retinal degeneration following vitrectomy in rabbits. *Sci Rep* 2019;9:15696.
9. Jang KH, Do YJ, Koo TS, et al. Protective effect of RIPK1-inhibitory compound in in vivo models for retinal degenerative disease. *Exp Eye Res* 2019;180:8-17.
10. Chowers G, Cohen M, Marks-Ohana D, et al. Course of Sodium Iodate-Induced Retinal Degeneration in Albino and Pigmented Mice. *Invest Ophthalmol Vis Sci* 2017;58:2239-49.
11. Kim SY, Assawachananont J. A New Method to Visualize the Intact Subretina From Retinal Pigment Epithelium to Retinal Tissue in Whole Mount of Pigmented Mouse Eyes. *Transl Vis Sci Technol* 2016;5:6.
12. Liu J, Li J, Chen Z, et al. Anisometric Amblyopia: Interocular Contrast and Viewing Luminance Effects on Aniseikonia. *Transl Vis Sci Technol* 2020;9:11.
13. Kim HL, Nam SM, Chang BJ, et al. Ultrastructural Changes and Expression of PCNA and RPE65 in Sodium Iodate-Induced Acute Retinal Pigment Epithelium Degeneration Model. *Neurochem Res* 2018;43:1010-9.
14. Yang Y, Ng TK, Ye C, et al. Assessing sodium iodate-induced outer retinal changes in rats using confocal scanning laser ophthalmoscopy and optical coherence tomography. *Invest Ophthalmol Vis Sci* 2014;55:1696-705.
15. Lee SJ, Kim SY. Non-separate Mouse Sclerochoroid/RPE/Retina Staining and Whole Mount for the Integral Observation of Subretinal Layer. *Bio Protoc* 2021;11:e3872.
16. Curcio CA, Zanzottera EC, Ach T, et al. Activated Retinal Pigment Epithelium, an Optical Coherence Tomography Biomarker for Progression in Age-Related Macular Degeneration. *Invest Ophthalmol Vis Sci* 2017;58:BIO211-26.
17. Schuman SG, Koreishi AF, Farsiu S, et al. Photoreceptor layer thinning over drusen in eyes with age-related macular degeneration imaged in vivo with spectral-domain optical coherence tomography. *Ophthalmology* 2009;116:488-496.e2.
18. Wang J, Iacovelli J, Spencer C, et al. Direct effect of sodium iodate on neurosensory retina. *Invest Ophthalmol Vis Sci* 2014;55:1941-53.
19. Dunaief JL, Dentchev T, Ying GS, et al. The role of apoptosis in age-related macular degeneration. *Arch Ophthalmol* 2002;120:1435-42.
20. Milam AH, Jacobson SG. Photoreceptor rosettes with blue cone opsin immunoreactivity in retinitis pigmentosa. *Ophthalmology* 1990;97:1620-31.
21. Tulvatana W, Adamian M, Berson EL, et al. Photoreceptor rosettes in autosomal dominant retinitis pigmentosa with reduced penetrance. *Arch Ophthalmol* 1999;117:399-402.
22. Bhutto IA, Ogura S, Baldeosingh R, et al. An Acute Injury Model for the Phenotypic Characteristics of Geographic Atrophy. *Invest Ophthalmol Vis Sci* 2018;59:AMD143-51.

doi: 10.21037/aes-21-27

**Cite this article as:** Kim SY, Zhao Y, Kim HL, Oh Y, Xu Q. Sodium iodate-induced retina degeneration observed in non-separate sclerochoroid/retina pigment epithelium/retina whole mounts. *Ann Eye Sci* 2022;7:3.

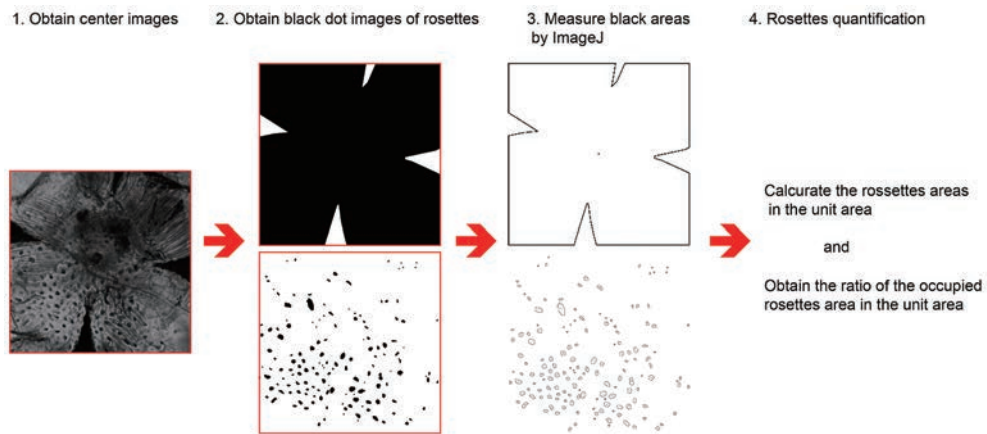


**Figure S1** Quantification of ONL rosettes in sclerochoroid/RPE/retina whole mounts. An example of the selected center area of ONL tiled retina (step1). The retinal region and the selected rosettes were colored black in each layer of white background (step2). The retina area and total areas of black dots of rosettes were measured by analyzing particles in ImageJ (step3). The rosettes areas in the defined retina unit were calculated based on the total rosettes and actual retinal areas, and the area ratios of the occupied rosettes in the unit retina were obtained for rosette quantification (step4). ONL, outer nuclear layer; RPE, retinal pigment epithelium.

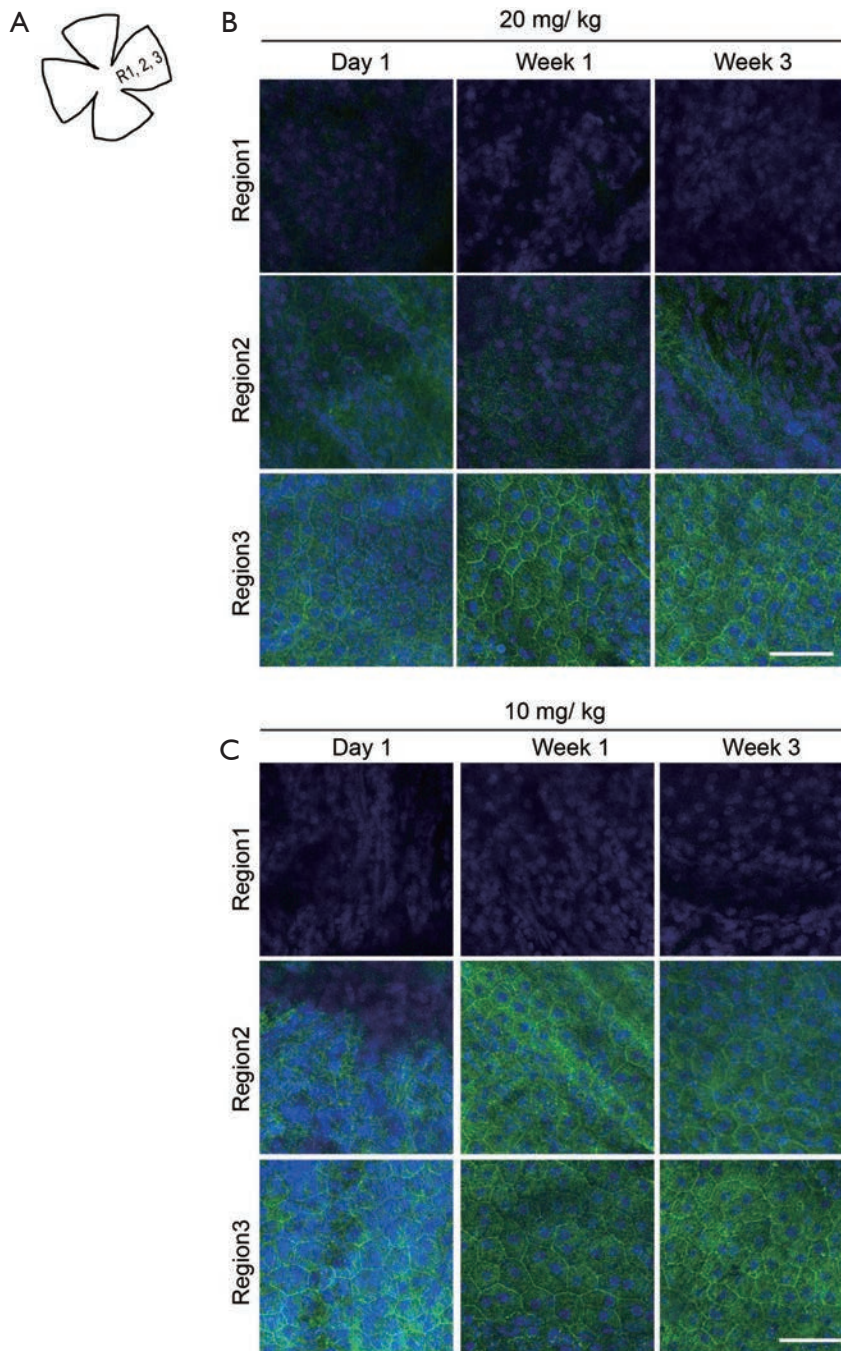


**Figure S2** RPE degeneration in horizontal view of whole mounts. SI (10, 20 mg/kg, i.p.)-induced RPE degeneration in BALB/C mice. (A) A schematic drawing of quadrant whole mount with regions indicated from center (R1) to peripheral region (R3). BALB/C mice were injected with 20 mg/kg SI (B) and 10 mg/kg SI (C). Sclerochoroid/RPE/retina whole mounts were stained with Alexa 488-conjugated phalloidin and Hoechst 33342. Images were taken in RPE layers from center (R1) to peripheral (R3) retinas at Day 1, Week 1 and Week 3. Scale bars: 50  $\mu$ m. RPE, retinal pigment epithelium; SI, sodium iodate.

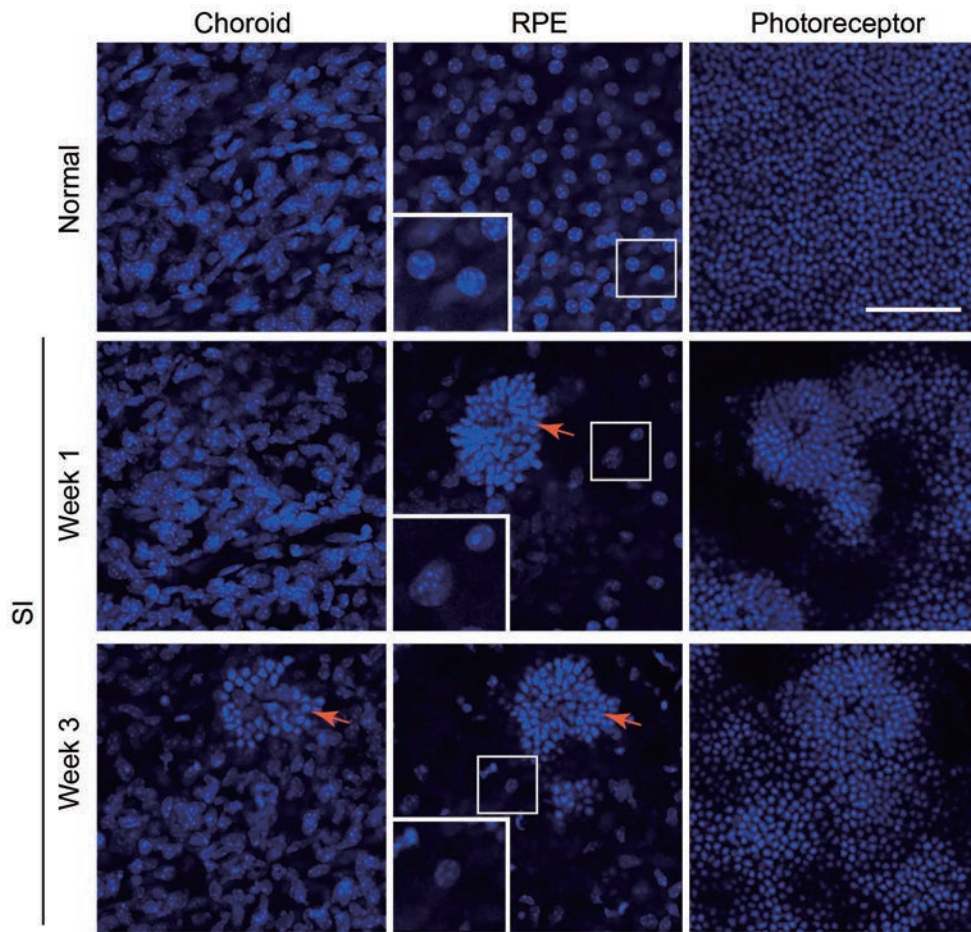


**Figure S3** SI-induced ocular damage at the level of choroid, RPE and PR layers in C57BL/6J sclerochoroid/RPE/retina whole mounts stained with Hoechst 33342. SI (50 mg/kg, i.p.)-induced retina degeneration in C57BL/6J mice. PR rosettes (arrows) and RPE nuclei (boxed areas). Inserts contain higher magnification of RPE nuclei in the boxed areas. Scale bar: 50  $\mu$ m. RPE, retinal pigment epithelium; SI, sodium iodate; PR, photoreceptor.